International Academy of Science, Engineering and Technology
Connecting Researchers; Nurturing Innovations
IASET

RATE ANALYSIS OF MASSIVE MIMO SYSTEM USING
STOCHASTIC GEOMETRIC MODEL

SHICHAOFENG, SIHANLUO & TIANLICUI

Beijing University of Technology, Beijing, P. R. China, China

ABSTRACT

The rate performance of massive multiple input multiple output (MIMO) system has been analyzed in the hexagonal model with deterministically placed users, which is too idealized and lacks rigorous theoretical analysis. This paper focuses on the downlink rate performance analysis on the massive MIMO system. Two general stochastic geometric models are employed owing to their tractability, i.e., Gilbert disk model and Voronoi tessellation model. Expressions for downlink average ergodic rate are derived in the general case and then simplified in the special case with definite path loss exponent. The simulation results of both models show that increasing the number of available pilots in each cell and the ratio of base stations (BS) density to user equipment (UE) density can improve the downlink average rate per UE. Furthermore, we compare the downlink rate results in these two models and observe that, pilot contamination in the Gilbert disk model is severer than that in the Voronoi tessellation model.

KEYWORDS: Massive MIMO, Stochastic Geometric Model, Pilot Contamination, Average Achievable Rate, Wireless Network

I. INTRODUCTION

In massive multiple input multiple output (MIMO) system, the base station (BS) employs antenna arrays with an order of magnitude more elements than the total number of serving single-antenna user equipments (UEs). In recent years, massive MIMO attracts broad attention because it can improve the transmission rate significantly and save, transmit power by an order of magnitude [1] –[3]. Massive MIMO has also been regarded as one of the most promising technologies in future wireless communication system.

Average rate indicates the performance of wireless communication system. In massive MIMO system, the large scale antenna array at BS is assumed to be equipped with unlimited numbers of antenna elements theoretically [3] –[5]. Under such assumptions, the effect of uncorrelated noise vanishes because of the law of large numbers. The remaining impairment is inter-cellular interference caused by reuse of pilot sequences in other cells, which is called pilot contamination [6] –[8]. In addition, with unlimited numbers of antennas, the effect of small scale fading also disappears. Accordingly, only the effect of large scale fading remains in propagation. To sum up, the rate performance of the massive MIMO system depends on pilot contamination and large scale fading.

The main contributions of this paper are described below. Firstly, we discuss the downlink average rate of a typical UE in the massive MIMO system in Section III, using a stochastic geometric model. Expressions for downlink average ergodic rate are derived in the general case and then they are simplified in the special case with definite path loss exponent. These expressions which involve quickly computable integrals are essential to further study the downlink rate performance of the massive MIMO system. Secondly, in Section IV, our analysis demonstrates that the downlink rate

performance per UE can be improved by increasing the ratio of BS density to UE density or the number of available pilots in each cell. This is distinct from the conventional cellular system where BS density doesn't impact interference-limited ergodic capacity per UE in downlink [9]. In addition, the downlink rate results of both Gilbert disk model and Voronoi tessellation model are compared. The reason for their difference is analyzed in detail. Simulation results show that the average pilot reuse probability in the Gilbert disk model is greater than that in the Voronoi tessellation model.

II. SYSTEM MODEL

The cellular system consists of BSs arranged according to the homogeneous Poisson point process (PPP) with the density λ_b. Each BS is equipped with a large scale antenna array, containing M ($M \to \infty$) antenna elements. The density of UEs is λ_u. The network adopts the Δ-frequency reuse scheme where $\Delta = 1,2,3$ etc. And there are P orthogonal pilot sequences available in each cell, which means that the maximum number of UEs served by one BS is P. All BSs share these finite pilots. In addition, the time division duplexing (TDD) mode is employed. The path loss exponent is α ($\alpha > 2$) in propagation model.

Channel estimation aims at acquiring the channel vector between BS and its associated UE. In uplink time slot, a typical UE transmits a pilot sequence to its associated BS. BS accidentally receives signals from other UEs which share the same pilot. Assume that UE_{km} represents the UE which uses the mth pilot in the coverage area of kth BS (denoted as BS_k). Then the estimated channel vector of UE_{km} acquired by BS_k can be expressed as $\hat{\mathbf{h}}_{kkm} = \mathbf{h}_{kkm} + \sum_{l \neq k} \mathbf{h}_{klm} \mathcal{I}(m,l) + \mathbf{n}_k$, where $\mathbf{h}_{klm} = \sqrt{\beta_{klm} R_{klm}^{-\alpha}} \mathbf{g}_{klm}$; the channel vector between BS_k and UE_{lm}, $\mathbf{g}_{klm} \in \mathbb{C}^{M \times 1}$ is the small scale fading vector, β_{klm} and R_{klm} represent large scale fading and distance between the BS_k and the UE_{lm} respectively and $\mathbf{n}_k$ is additive zero-mean noise vector. β_{klm} is assumed to obey the exponential distribution. Such assumption is possible when the interference follows Rayleigh fading. $\mathrm{I}(m,l)$ is used to indicate whether the mth pilot is reused by BS_l, i.e., $\mathrm{I}(m,l) = 1$, when mth pilot is used in lth cell, 0 otherwise. After channel estimation, the downlink data transmission starts in the next downlink time slot. Assume that Maximum Ratio Transmission (MRT) is employed at BS which uses the conjugate transpose of estimated channel vector as the precoding vector. Then the received data symbol of UE_{km} can be calculated as,

$$s_{km} = \lim_{M \to \infty} \frac{y_{km}}{M\sqrt{\rho}} = \lim_{M \to \infty} \left[\sum_{l=1}^{\infty} \frac{\mathbf{h}_{lkm}\mathbf{x}_{lm}}{M} \mathcal{I}(m,l) + \frac{w_{km}}{M\sqrt{\rho}} \right] \overset{(a)}{=} \lim_{M \to \infty} \sum_{l=1}^{\infty} \frac{\mathbf{h}_{llm}^H \mathbf{h}_{llm}}{M} s_{lm} \mathcal{I}(m,l)$$

$$\overset{(b)}{=} \beta_{kkm} R_{kkm}^{-\alpha} s_{km} + \sum_{l=1, l \neq k}^{\infty} \beta_{lkm} R_{lkm}^{-\alpha} s_{lm} \mathcal{I}(m,l),$$

$$(1)$$

Where, ρ is the downlink signal-to-noise ratio (SNR), $y_{km} = \sqrt{\rho} \sum_{l=1}^{\infty} \mathbf{h}_{lkm}\mathbf{x}_{lm}\mathcal{I}(m,l) + w_{km}$ is the received signal of UE_{km}, $\mathbf{x}_{lm} = \hat{\mathbf{h}}_{llm} s_{lm}$ is the signal transmitted by BS_l, s_{lm} is the data symbol desired by UE_{lm} and w_{km} is the additive zero-mean noise. (a) Is obtained by noting that the correlation of different channel vectors tends to be zero as $M \to \infty$. (b) Follows from the law of large numbers. In addition, the effect of small scale fading disappears as $M \to \infty$ [3]. Then the downlink signal-to-interference ratio (SIR) of UE_{km} can be expressed as

$$SIR_{km} = \frac{\beta_{kkm} R_{kkm}^{-\alpha}}{I_{km}}, \quad I_{km} = \sum_{l=1, l \neq k}^{\infty} \beta_{lkm} R_{lkm}^{-\alpha} \mathcal{I}(m,l)$$

$$(2)$$

III. AVERAGE ACHIEVABLE RATE

In this section, we will discuss the downlink average achievable rate. At first, we focus on the probability of using the same pilot between two BSs in the system. The overhead is not taken into consideration in this paper. The average pilot reuse probability can be expressed as $\eta = \mathbb{E}\left[\mathcal{I}(m, l)\right] = \sum_{n=0}^{P-1} \frac{n}{P} \mathbb{P}\left[N = n\right] + \sum_{n=P}^{\infty} \mathbb{P}\left[N = n\right]$, where N is the number of UEs in the coverage area of a typical BS and $\mathbb{P}\left[N = n\right]$ is the probability density function (PDF) of the number of UEs in the coverage area of a BS. Combining (2) with (2), the average ergodic rate of a typical mobile user in the downlink can be calculated as,

$$
\begin{aligned}
\tau(\lambda_b, \alpha) &= \mathbb{E}[\ln(1 - SIR_{km})] = \mathbb{E}_{\{t_{kkn}, I_{km}, \beta_{kkm}\}} \left[\ln\left(1 - \frac{\beta_{kkm} R_{kkm}^{-\alpha}}{I_{km}}\right)\right] \\
&= \int_{r \in \Psi} f_{R_{kkm}}(r) \mathbb{E}_{I_{km}, \beta_{kkm}} \left[\ln\left(1 + \frac{\beta_{kkm} r^{-\alpha}}{I_{km}}\right)\right] \mathrm{d}r \\
&\overset{(a)}{=} \int_{r \in \Psi} f_{R_{kkm}}(r) \int_{t > 0} \mathcal{L}_{I_{km}}\left[(e^t - 1)r^\alpha\right] \mathrm{d}t \mathrm{d}r,
\end{aligned}
$$

(3)

Where, f_{Rkkm} (r) is R_{kkm}'s PDF, Ψ is the set of distances between UE and its associated BS and L $(\cdot)$ returns the Laplace transform. Assume that the large scale fading β_{kkm} follows the exponential distribution with mean 1. (a) Follows from the proof of theorem 3 in Appendix C of [9]. R_{kkm}'s PDF and set Ψ depend on the employed stochastic geometric model. Next we'll present the expressions of average achievable rate using two different stochastic geometric models.

A. Gilbert Disk Model

Gilbert disk model comes from Gilbert's random disk graph [10], which is a special case of Boolean models [11]. In the Gilbert disk model, the coverage area of BS is assumed to be a disk of radius R centered at the BS, which is shown in Figure 1. UEs are uniformly distributed on the circle. As is shown in Figure 1, such cell deployment inevitably results in overlap of different cells.

But, the Gilbert disk model ensures that each BS is at the center of each cell. And the real cell coverage area approximates a circle. The number of UEs served by a given BS is a Poisson random variable with mean $\lambda_u \pi R^2$ where λ_u is the density of UE, i.e., $\mathbb{P}_D\left[N = n\right] = \frac{\left(\lambda_u \pi R^2\right)^n}{n!} e^{-\lambda_u \pi R^2}$, where $n = 0, 1, 2$ etc. The average pilot reuse probability in this model can be expressed as $\eta_D = \sum_{n=0}^{P-1} \frac{n}{P} \mathbb{P}_D\left[N = n\right] + \sum_{n=P}^{\infty} \mathbb{P}_D\left[N = n\right]$. Since UEs are uniformly distributed in each cell, the PDF of R_{kkm} is
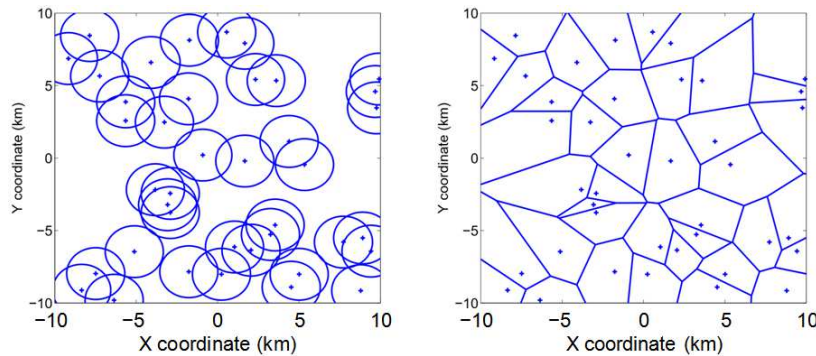
Figure 1: Top Arrangement of BSs Using Gilbert Disk Model, Each Cell Coverage Area is a Circle
Button: Arrangement of BSs Using Voronoi Tessellation Model, the Cell Boundaries form a Voronoi Tessellation

$$f^D_{R_{kkm}}(r) = \frac{2r}{R^2}, \qquad 0 \le r \le R$$, where R is the coverage radius. Assume that the variable β_{lkm} follows an exponential distribution with mean 1, i.e., $\beta_{lkm} \sim$ exp (1). According to the definition of the Laplace transform,

$$
\begin{aligned}
\mathcal{L}^D_{I_{km}}(s) &= \mathrm{E}_{I_{km}}\left[e^{-sI_{km}}\right] \overset{(a)}{=} \mathrm{E}_{\phi,\beta}\left[\eta_D \prod_{l \in \Phi \backslash k} \exp(-s\beta P_{lkm} r^{-\alpha})\right] \overset{(b)}{=} \exp\left(-\frac{\lambda_b \eta_D}{\Delta}\int_0^\infty \mathrm{E}_\beta\left[1 - e^{-s\beta r^{-\alpha}}\right]2\pi r dr\right) \\
&\overset{(c)}{=} \exp\left(-\pi\lambda^D_{eff} s^{\frac{2}{\alpha}} \mathrm{E}\left[\beta^{\frac{2}{\alpha}}\right]\int_0^\infty\left(1 - e^{-t}\,\tfrac{2}{\alpha}\right)dt\right) \overset{(d)}{=}\exp\left[\frac{2\pi\lambda^D_{eff} s^{\frac{2}{\alpha}}}{\alpha}\Gamma\left(\frac{2}{\alpha}+1\right)\Gamma\left(-\frac{2}{\alpha}\right)\right] \\
&\overset{(e)}{=} \exp\left(-\frac{\pi\lambda^D_{eff} s^{\frac{2}{\alpha}}}{\mathrm{sinc}\left(\frac{2\pi}{\alpha}\right)}\right).
\end{aligned}
$$

(4)

Where, Φ denotes the set of all BSs. (a) is evaluated by $\eta_D = \mathrm{E}[I(m,l)]$ and the substitution $\beta_{lkm} \to \beta$. (b) follows from the probability generating functional (PGFL) of PPP [12]. (c) Is evaluated by using the change of variable $s^{-\frac{2}{\alpha}}\beta^{-\frac{2}{\alpha}}v^2 \to t$. Note that $\lambda^D_{eff} = \lambda_b\eta_D/\Delta$ represents the effective interfering BS density. The interfering BS transmits signal to its associated UE which shares the same pilot with the desired UE in target cell. (d) Follows from the definition of gamma function. (e) Follows from Euler's reflection formula $\Gamma(z)\Gamma(1-z) = \frac{\pi}{\sin(\pi z)}$. Using the substitution $\frac{\pi\lambda_{eff}}{\mathrm{sinc}\left(\frac{2\pi}{\alpha}\right)} \to T_D$, the expression can be rewritten as $\mathcal{L}^D_{I_{km}}(s) = \exp\left(-T_D s^{\frac{2}{\alpha}}\right)$. Plugging it in (3), the average achievable rate can be calculated as

$$
\begin{aligned}
\tau_D(\lambda_b, \alpha) &= \int_0^R\int_0^\infty \exp\left[-T_D\left(e^t - 1\right)^{\frac{2}{\alpha}} r^2\right]\frac{2r}{R^2}dtdr = \frac{1}{T_D R^2}\int_0^\infty\frac{1 - \exp\left[-T_D\left(e^t - 1\right)^{\frac{2}{\alpha}}R^2\right]}{\left(e^t - 1\right)^{\frac{2}{\alpha}}}dt \\
&\overset{(a)}{=}\frac{\alpha}{T_D R^2}\int_0^\infty\frac{\left(1 - e^{-T_D R^2 x^2}\right)x^{\alpha-3}}{x^\alpha + 1}dx,
\end{aligned}
$$

(5)

B. Voronoi Tessellation Model

The Voronni tessellation model is developed for multi-cell system in [9]. In the Voronoi tessellation model, each UE is assumed to be distributed according to an independent PPP with density λ_u and associated with its closest BS. The cell boundaries form a Voronoi tessellation, which is shown in Figure 1. No overlap between coverage areas of different BSs exists. In reality, each UE is associated with its closest BS so that the path loss between the UE and its associated BS is the least. Nevertheless, BSs in the model may be located so closely together, but with a significant coverage area in Voronoi tessellation model [9]. In addition, the UE has access to real network if its received power is larger than a threshold. But UE in the model may be so isolated that the received power from its closest BS cannot satisfy the requirement.

According to [13], the probability density function of the number of UEs in the coverage area of a BS is

$$
\mathbb{P}_V[N = n] = \frac{3.5^{3.5}\Gamma(n + 3.5)(\lambda_u/\lambda_b)^n}{\Gamma(3.5)n!(\lambda_u/\lambda_b + 3.5)^{n+3.5}},
$$

(6)

where $n = 0, 1, 2$ etc. Then the average pilot reuse probability can be rewritten as

$$
\eta_V = \sum_{n=0}^{P-1}\frac{n}{P}\mathbb{P}_V[N = n] + \sum_{n=P}^\infty \mathbb{P}_V[N = n].
$$

(7)

Since each UE associate with its closest BS, the PDF of R_{kkm} can be calculated as [9]

$$f^V_{R_{lkm}}(r) = e^{-\lambda_b \pi r^2} 2\pi \lambda_b r, \qquad r \in [0, +\infty).$$

(8)

Assume that the variable β_{lkm} follows an exponential distribution with mean 1, i.e., $\beta_{lkm} \sim$ exp (1). Then the Laplace transform of I_{km} can be rewritten as,

$$\mathcal{L}^V_{I_{km}}(s) = \mathbb{E}_{\Phi,\beta}\left[\prod_{l \in \Phi \backslash k} \exp\left(-s\beta R^{-\alpha}_{lkm}\mathcal{I}(m,l)\right)\right] = \mathbb{E}_{\Phi}\left[\prod_{l \in \Phi \backslash k} \mathbb{E}_{\beta}\left[\exp\left(-s\beta R^{-\alpha}_{lkm}\right)\right]\mathcal{I}(m,l)\right]$$

$$= \mathbb{E}_{\Phi}\left[\prod_{l \in \Phi \backslash k} \frac{1}{1 + sR^{-\alpha}_{lkm}}\mathcal{I}(m,l)\right] = \exp\left[-\int_r^\infty \left(1 - \frac{1}{1 + sr'^{-\alpha}}\right)2\pi\lambda^V_{eff}\,r'\,\mathrm{d}r'\right],$$

Where, $\lambda^V_{eff} = \lambda_b \eta_V / \Delta$ is the effective interfering BS density. The technical tools are similar to Subsection A, so the discussion will be more concise. According to Appendix C in [9],

$$\mathcal{L}^V_{I_{km}}((e^t - 1)r^\alpha) = \exp\left(-\pi\lambda^V_{eff} r^2 (e^t - 1)^{\frac{2}{\alpha}} \int_{(e^t-1)^{-\frac{2}{\alpha}}}^\infty \frac{1}{1 + x^{\alpha/2}}\mathrm{d}x\right)$$

(9)

The average achievable rate can be calculated as,

$$\tau_V(\lambda_b, \alpha) = \int_0^\infty \int_0^\infty e^{-\lambda_b \pi r^2 \left[\frac{\eta_V}{\Delta}(e^t-1)^{\frac{2}{\alpha}}\int_{(e^t-1)^{-\frac{2}{\alpha}}}^\infty \frac{1}{1+x^{\alpha/2}}\mathrm{d}x + 1\right]}\mathrm{d}(\pi\lambda_b r^2)\mathrm{d}t$$

$$= \int_0^\infty \frac{\Delta}{\eta_V(e^t-1)^{2/\alpha}\int_{(e^t-1)^{-2/\alpha}}^\infty \frac{1}{1+x^{\alpha/2}}\mathrm{d}x + \Delta}\mathrm{d}t.$$

(10)

IV. NUMERICAL ANALYSIS

In this section, the average pilot reuse probability will be discussed at first. Then the downlink rate performance of the massive MIMO system will be analyzed in detail. Considering the expressions of average achievable rate, both of them seem to be irrelevant to BS density. As is derived in [9], the expression of interference-limited ergodic capacity per user doesn't depend on BS density. However, the BS density actually impacts the average achievable rate by affecting the average pilot reuse probability η_D and η_V in the massive MIMO system. In order to express the rate in bps/Hz, the results of (??) and (??) divide by ln2. The downlink average achievable rates in both models are plotted with respect to the ratio of UE density to BS density λ_u/λ_b in Figure 2. Firstly, the average achievable rates decline with λ_u/λ_b. Crowded UEs in the coverage area of each BS will result in high pilot reuse probability which then leads to intense interference from pilot contamination. And increasing available pilots per cell can relieve the pilot contamination. Moreover, with a finite number of pilots, the rate performance in a Voronoi tessellation model is worse than that in the Gilbert disk model if λ_u/λ_b is smaller than the threshold (approximately equal to $P/2$). It means that the system in Gilbert disk model achieves better performance if dense cells are deployed. But for λ_u/λ_b larger than that threshold, the rate performance in a Voronoi tessellation model exceeds that in the Gilbert disk model. That's because the system in Gilbert disk model leads to higher average pilot reuse probability if λ_u/λ_b is larger than $P/2$. In the case $\Delta = 1$, The lower limit of downlink average achievable rate in the Voronoi tessellation model is 2.15 bps/Hz, while that in the Gilbert disk model is 2.02 bps/Hz.
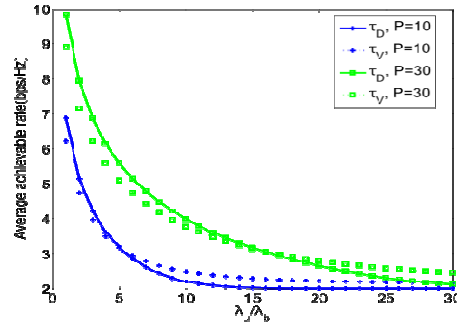
Figure 2: Average Achievable Rate τD and τV vs. $\lambda u/\lambda_b$ for the number of Available Pilots, P =10, 30 Respectively, where the Frequency Reuse Factor Δ=1 and Path Loss Exponent α =4

V. CONCLUSIONS

This paper discusses the downlink rate performance of the massive MIMO system. Two general stochastic geometric models are employed, i.e., Gilbert disk model and Voronoi tessellation model. Expressions of downlink average ergodic rate are derived in these two models, respectively. Simulation results show that the downlink average rate in the massive MIMO system increases with the ratio of BS density to UE density and the number of available pilots in each cell. In addition, the rate performances of these two models are compared. Simulation results also show that the average pilot reuse probability in the Gilbert disk model is greater than that in the Voronoi tessellation model.

REFERENCES

1. E. G. Larsson, F. Tufvesson, O. Edfors, and T. L. Marzetta, "Massive MIMO for next generation wireless systems," *Communications Magazine, IEEE*, vol. 52, no. 2, pp. 186–195, 2014.

2. H. Q. Ngo, E. G. Larsson, and T. L. Marzetta, "Energy and spectral efficiency of very large multiuser MIMO systems," *Communications, IEEE Transactions on*, vol. 61, no. 4, pp. 1436–1449, 2013.

3. F. Rusek, D. Persson, B. K. Lau, E. G. Larsson, T. L. Marzetta, O. Edfors, and F. Tufvesson, "Scaling up MIMO: Opportunities and challenges with very large arrays," *Signal Processing Magazine, IEEE*, vol. 30, no. 1, pp. 40–60, 2013.

4. J. Hoydis, S. Ten Brink, M. Debbah*et al.*, "Massive MIMO in the UL/DL of cellular networks: How many antennas do we need?" *Selected Areas in Communications, IEEE Journal on*, vol. 31, no. 2, pp. 160–171, 2013.

5. P. Madhusudhanan, X. Li, Y. Liu, and T. X. Brown, "Stochastic geometric modeling and interference analysis of massive MIMO systems," in *Modeling & Optimization in Mobile, Ad Hoc & Wireless Networks (WiOpt), 2013 11th International Symposium on*. IEEE, 2013, pp. 15–22.

6. T. L. Marzetta, "Noncooperative cellular wireless with unlimited numbers of base station antennas," *Wireless Communications, IEEE Transactions on*, vol. 9, no. 11, pp. 3590–3600, 2010.

7. J. Jose, A. Ashikhmin, T. L. Marzetta, and S. Vishwanath, "Pilot contamination and precoding in multi-cell TDD systems," *Wireless Communications, IEEE Transactions on*, vol. 10, no. 8, pp. 2640–2651, 2011.

8. F. Fernandes, A. E. Ashikhmin, and T. L. Marzetta, "Inter-Cell Interference in Noncooperative TDD Large Scale Antenna Systems," *Selected Areas in Communications, IEEE Journal on*, vol. 31, no. 2, pp. 192–201, 2013.

9. J. G. Andrews, F. Baccelli, and R. K. Ganti, "A tractable approach to coverage and rate in cellular networks," *Communications, IEEE Transactions on*, vol. 59, no. 11, pp. 3122–3134, 2011.

10. E. N. Gilbert, "Random plane networks," *Journal of the Society for Industrial & Applied Mathematics*, vol. 9, no. 4, pp. 533–543, 1961.

11. M. Haenggi, J. G. Andrews, F. Baccelli, O. Dousse, and M. Franceschetti, "Stochastic geometry and random graphs for the analysis and design of wireless networks," *Selected Areas in Communications, IEEE Journal on*, vol. 27, no. 7, pp. 1029–1046, 2009.

12. M. Haenggi and R. K. Ganti, *Interference in large wireless networks*. Now Publishers Inc, 2009.

13. S. M. Yu and S. L. Kim, "Downlink capacity and base station density in cellular networks," in *Modeling & Optimization in Mobile, Ad Hoc & Wireless Networks (WiOpt), 2013 11th International Symposium on*. IEEE, 2013, pp. 119–124.